



**HAL**  
open science

# The impact of the particle size distribution of organic additives on the microstructure of a clay ceramic and its thermal and mechanical properties

Pierre-Marie Nigay, Ange Nzihou, Thierry Cutard

## ► To cite this version:

Pierre-Marie Nigay, Ange Nzihou, Thierry Cutard. The impact of the particle size distribution of organic additives on the microstructure of a clay ceramic and its thermal and mechanical properties. *Journal of Materials in Civil Engineering*, 2018, 30 (4), pp.04018044. 10.1061/%28ASCE%29MT.1943-5533.0002221 . hal-01701896

**HAL Id: hal-01701896**

**<https://hal.science/hal-01701896>**

Submitted on 28 Feb 2019

**HAL** is a multi-disciplinary open access archive for the deposit and dissemination of scientific research documents, whether they are published or not. The documents may come from teaching and research institutions in France or abroad, or from public or private research centers.

L'archive ouverte pluridisciplinaire **HAL**, est destinée au dépôt et à la diffusion de documents scientifiques de niveau recherche, publiés ou non, émanant des établissements d'enseignement et de recherche français ou étrangers, des laboratoires publics ou privés.

# The Impact of the Particle Size Distribution of Organic Additives on the Microstructure of a Clay Ceramic and Its Thermal and Mechanical Properties

Pierre-Marie Nigay<sup>1</sup>; Ange Nzihou<sup>2</sup>; and Thierry Cutard<sup>3</sup>

**Abstract:** In this study, the structure-property relationships of a clay ceramic with calibrated particles (10 or 50  $\mu\text{m}$ ) of polymethyl methacrylate (PMMA) were investigated to improve both the thermal and mechanical properties of fired clay bricks incorporating organic wastes. The structure was characterized using differential thermal, thermomechanical, and computed tomography analysis. It was found that the addition of 10- or 50- $\mu\text{m}$  particles of PMMA resulted in a same 11% decrease of the thermal conductivity during the extrusion process. The Young's modulus also increased by 23% during the extrusion process with the addition of 50- $\mu\text{m}$  particles. However, the addition of 10- $\mu\text{m}$  particles resulted in a greater increase of the Young's modulus by 34%. The calibrated particles of PMMA were then found to transform into porosity during firing of the clay ceramic. Typically, the pore size of the clay ceramic corresponded to the particle size of the calibrated particles of PMMA. The improvement of the thermal and mechanical properties that was obtained during the extrusion process was conserved in the form of porosity with a reduction of the median pore size after the firing process. Hence, the current results indicate that the thermal and mechanical properties of fired clay bricks can be improved at the same time using a wide range of organic wastes if the organic wastes are subjected to grinding prior to incorporation in the mixture. They also suggest that organic wastes can reduce the environmental impact of fired clay bricks with an energetic contribution of 73.8%.

**Author keywords:** Clay bricks; Organic additives; Porosity; Thermal conductivity; Young's modulus; Energetic contribution.

## Introduction

The recycling of industrial and urban waste has recently gained momentum in the field of building materials (Zhang 2013; Bories et al. 2014). The addition of waste to the composition of fired clay bricks has positive effects on the performances. Moreover, waste is a potential energy carrier in the industrial process of fired clay bricks.

The waste comes from wood, paper, or oil industries. It is mostly used for the high organic fraction beyond 60% (Phonphuak and Chindaprasit 2014). The addition ranges from 1 to 30% depending on the organic fraction (Monteiro and Vieira 2014). On the other hand, the particle size ranges from 1 to 4 mm to keep the process unchanged (Andreola et al. 2001).

The organic additives are then subjected to combustion during firing of the clay bricks at temperatures up to 1,000°C (Demir 2008). The combustion of these organic additives also results in

a porosity formation within the bricks. Hence, the clay bricks have a higher volume fraction of pores after the firing process (Muñoz Velasco et al. 2015).

The insulating behavior of air in the newly formed pores improves the thermal properties of the fired clay bricks (Dondi et al. 2004; Mendivil et al. 2017). It has been shown that the porosity resulting from the combustion of waste from oil industry decreased the thermal conductivity by 20% (Eliche-Quesada et al. 2012). The thermal conductivity also decreased by 36% in another study where sawdust was used as the pore-forming agent (Bánhidi and Gömze 2008). However, that improvement of the thermal conductivity is always obtained along with a loss in the mechanical strength (Bories et al. 2015). Typically, these pores resulting from the combustion of organic additives are acting like defects (Ukwatta and Mohajerani 2017). It has been shown that the mechanical strength of fired clay bricks decreased by 4% when using sludge from wastewater treatment as the pore-forming agent (Monteiro et al. 2008). Some other studies also revealed that the pores resulting from the combustion of sawdust can result in a critical loss of 27% (Ducman and Kopar 2001).

The combustion of the organic additives results in an extensive release of heat within the tunnel kilns. The temperature increase provides an energetic contribution to the process and energy savings. According to the literature, the energy savings can reach up to 58% using a 5% by weight addition of cigarette butts (Mohajerani et al. 2016). The recycling of industrial and urban waste in fired clay bricks is then a relevant concept. It provides an improvement of the thermal properties as well as energy savings. The loss of strength is a major issue for such materials. However, Korah et al. (2016) have shown in a recent study that the addition of organic additives with smaller particles can result in the formation of smaller pores. These small pores resulting from the combustion of the organic additives may act as minor defects and prevent the loss

---

<sup>1</sup>Postdoctoral Researcher, Centre Recherche d'Albi en génie des Procédés des Solides Divisés, de l'Énergie et de l'Environnement, Ecole des Mines d'Albi, Campus Jarlard, Route de Teillet, 81013 Albi Cedex 09, France (corresponding author). ORCID: <https://orcid.org/0000-0003-2204-6205>. E-mail: pierre-marie.nigay@mines-albi.fr

<sup>2</sup>Professor, Centre Recherche d'Albi en génie des Procédés des Solides Divisés, de l'Énergie et de l'Environnement, Ecole des Mines d'Albi, Campus Jarlard, Route de Teillet, 81013 Albi Cedex 09, France. E-mail: ange.nzihou@mines-albi.fr

<sup>3</sup>Professor, Institut Clément Ader, Ecole des Mines d'Albi, Campus Jarlard, Route de Teillet, 81013 Albi Cedex 09, France. E-mail: thierry.cutard@mines-albi.fr

of strength, as shown by Nigay et al. (2017) for the small pores resulting from mineralogical transformations of the clay.

The objective of this study is to investigate the impact of the particle size distribution of organic additives on the microstructure of a clay ceramic and its thermal and mechanical properties. Hence, the study focuses on a 6% by weight addition of a same organic additive in one form of 10- $\mu\text{m}$  particles and one form of 50- $\mu\text{m}$  particles. The particle size distribution is compared with the pore size distribution. The volume fraction and the size of the newly formed pores are also related to the evolution of the thermal conductivity and of the Young's modulus during the firing process. Therefore, the study should provide a useful insight into how the microstructure of fired clay bricks can be controlled by the particle size distribution of organic additives to improve both the thermal and mechanical properties.

## Materials and Methods

### Raw Materials

The clay was extracted from a quarry in the Toulouse area (France). The lumps of clay were ground into smaller lumps of approximately 3 mm using a rolling mill (LA 1527, Vicentini, Cavazzale, Italy). The composition, measured via inductively coupled plasma-atomic emission spectroscopy (ICP-AES) (Ultima 2, Jobin Yvon, Longjumeau, France), showed a predominance of silicon and aluminum oxides with smaller concentrations of calcium, iron, and potassium oxides.

The organic additives consisted of a thermoplastic polymer of polymethyl methacrylate (PMMA). They were obtained from Microbeads Company (Skedsmokorset, Norway) in the form of 10- ( $\text{MB}_{10}$ ) and 50- $\mu\text{m}$  ( $\text{MB}_{50}$ ) microbeads. The elemental composition that was determined using organic elemental analysis (Flash 2000, Thermo Fisher Scientific, Waltham, Massachusetts) is summarized in Table 1. The results show that the  $\text{MB}_{10}$  and  $\text{MB}_{50}$  additives had the same composition. They were both composed of organic elements such carbon, oxygen, and hydrogen with a minor amount of nitrogen.

The heating value of the organic additives was measured using an oxygen bomb calorimeter (C 6000, IKA, Wilmington, North Carolina). The measurements were performed under adiabatic mode with pill samples that were compressed in a press machine. The lower heating value of the organic additives was estimated by subtracting the latent heat of vaporization from the results of the higher heating value. The  $\text{MB}_{10}$  and  $\text{MB}_{50}$  additives both had a lower heating value of 23,291 J/g.

The particle size distribution of the organic additives was measured by laser granulometry analysis using a Malvern Mastersizer 3,000 instrument (Malvern, United Kingdom). The results in Fig. 1 confirm the particle size of the organic additives. The  $\text{MB}_{10}$  and  $\text{MB}_{50}$  additives had an average particle size of 10 and 50  $\mu\text{m}$ , respectively.

**Table 1.** Elemental Composition of the  $\text{MB}_{10}$  and  $\text{MB}_{50}$  Additives with the Concentrations in Carbon, Hydrogen, Oxygen, Nitrogen, and Sulfur Elements

Sample	Concentration (% by weight)				
	C	H	O	N	S
$\text{MB}_{10}$	59.9	7.7	32.2	0.2	0.0
$\text{MB}_{50}$	59.8	7.9	32.1	0.2	0.0

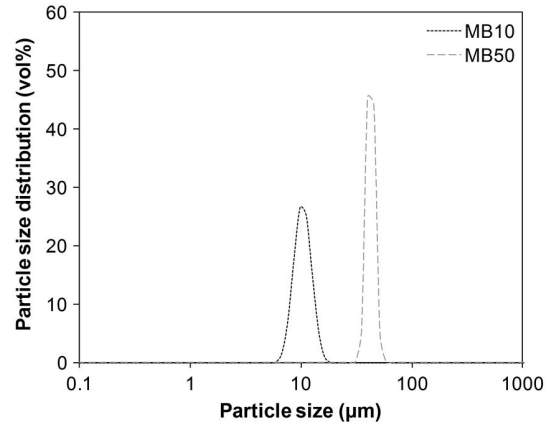


**Fig. 1.** Particle size distribution of  $\text{MB}_{10}$  and  $\text{MB}_{50}$  additives

### Processing of the Clay Ceramic

The clay ceramic was produced from different mixtures of clay with organic additives and water. The percentage of organic additives was determined from the results of Korah et al. (2016) to investigate the impact of the particle size distribution of the organic additives with yet an optimization of the percentage of addition for the thermal and the mechanical properties. Hence, the mixtures were prepared by mixing 10 kg of clay with 6% by weight of organic additives ( $\text{MB}_{10}$  or  $\text{MB}_{50}$ ). Some water was also added to the mixtures until an 800,000 Pa (8-bar) pressure of extrusion was obtained. Subsequently, the mixtures were extruded in the form of blocks with dimensions of  $180 \times 80 \times 18 \text{ mm}^3$  for a water content of 17% by weight. The blocks were dried at temperatures of 25, 65, and 105°C for 24 h. Finally, the different samples were prepared from the dried blocks using P80, P120, P180, and P280 SiC abrasive papers (Buehler, Uzwil, Switzerland). Some of the samples were also fired in a furnace (Controller P320, Nabertherm, Lilienthal, Germany) at temperatures given in the next sections.

### Characterization of the Microstructure

The mass loss and the heat flow of the clay ceramic were determined using differential thermal analyses (DTA). The unfired samples were analyzed in the form of 200-mg cylinders with a Setaram 92 apparatus (Caluire, France). The data were collected in air atmosphere at temperatures between 30 and 1,100°C using a 5°C/min heating rate.

The deformation was measured as a function of the temperature using thermomechanical analyses (TMA). The unfired samples were analyzed as 200-mg cylinders in a Setsys 16/18 instrument (Setaram, Caluire, France). The data were collected in air atmosphere at temperatures between 30 and 1,100°C (5°C/min heating rate). In fact, the DTA and TMA analyses were performed under the same conditions to provide an accurate estimate of the bulk density (Baillez and Nzihou 2004). The bulk density  $[\rho_{(T)}]$  was estimated from Eq. (1) using the mass loss, the shrinkage, the initial mass ( $m_0$ ), the initial length ( $l_0$ ), and the initial radius ( $r_0$ ) of the samples

$$\rho_{(T)} = \frac{m_0(1 - \text{MassLoss}_{(T)})}{\pi r_0^2 l_0 (1 - \text{Shrinkage}_{(T)})^3} \quad (1)$$

The dependence of the pore volume fraction on the firing temperature  $[\varepsilon_{(T)}]$  was estimated from Eq. (2) (Nigay et al. 2017). The estimates were obtained using the bulk density  $[\rho_{(T)}]$  and the true density of the particles ( $\rho_{\text{True}}$ ). The true density of the particles

was measured by Helium pycnometer analyses after firing at 1,100°C and grinding to remove the porosity. The value was equal to 2.72 g/cm<sup>3</sup>

$$\varepsilon_{(T)} = 1 - \frac{\rho_{(T)}}{\rho_{True}} \quad (2)$$

The three-dimensional (3D) representations of the porosity were obtained by X-ray tomography analysis using a Synchrotron facility (ESRF Grenoble). The samples were scanned in the form of 200-mg cylinders after firing at a temperature of 950°C.

### Determination of the Thermal Conductivity

The thermal conductivity was measured using a Hot Disk AB TPS 2500 system (Gothenburg, Sweden). The measurements were carried out with duplicate samples of 30 × 30 × 5 mm<sup>3</sup> after firing at 30, 200, 400, 600, 700, 800, 900, 1,000, and 1,100°C. In this way, the evolution of the thermal conductivity could be compared to the evolution of the volume fraction of pores with the firing temperature.

### Determination of the Young's Modulus and of the Flexural Strength

The Young's modulus was measured as a function of the temperature using a resonant frequency analyzer (RFDA HT650, IMCE, Genk, Belgium) with unfired samples of 60 × 30 × 5 mm<sup>3</sup>. The values of the Young's modulus were calculated from the fundamental frequency of resonance and the dimensions of the samples. They could be obtained in a continuous way at temperatures between 30 and 1,050°C.

The flexural strength was also measured using three-point bending tests after firing at a temperature of 950°C. The measurements were performed with flexural specimens of 60 × 30 × 5 mm<sup>3</sup>. The specimens were loaded in an Instron 5800R machine (Norwood, Massachusetts) with a 40-mm loading span and a 500-N load cell at a 1 mm/min displacement rate

$$\sigma_f = \frac{3F_{Max}L}{2BH^2} \quad (3)$$

The flexural strength of the clay ceramic ( $\sigma_f$ ) was estimated from Eq. (3), where  $F_{Max}$  is the maximum force,  $L$  is the loading span,  $B$  is the breadth, and  $H$  is the height of the samples (ASTM 2010).

### Determination of the Energetic Contribution

The energetic contribution of the organic additives was determined by DTA. The energy released by thermal degradation of the organic additives was estimated by integration of the exothermic peaks on the heat flow. The electrical value was transposed in an energetic value using a calibration with indium, tin, zinc, and aluminum standards. Furthermore, the energy required by the firing process of the clay ceramic was estimated by integration of the dehydration, dehydroxylation, and decarbonation peaks, in addition to the energy used to reach the temperature of 950°C. The energetic contribution was finally calculated as the quantity of energy released on the quantity of energy required.

## Results

### Thermal Behavior of the Clay Ceramic

The heat flow of the clay ceramic is presented in Fig. 2. The results show that the clay ceramic without organic additives is subjected to

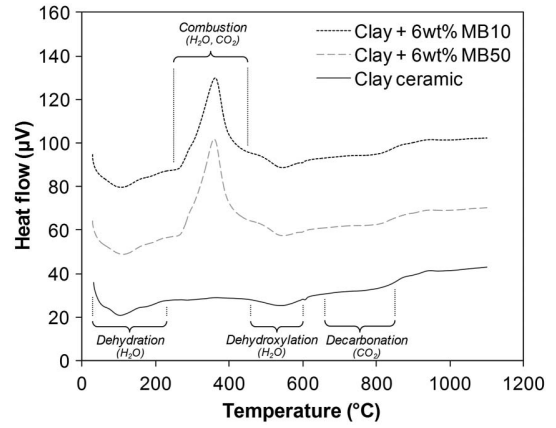


Fig. 2. Heat flow of the clay ceramic and of the clay ceramic with a 6% by weight addition of MB<sub>10</sub> and MB<sub>50</sub> additives

dehydration at temperatures between 30 and 200°C. The release of interposition water that remained in the pores, along with the release of hygroscopic water that was absorbed on the clay particles, involves a 304 J/g absorption of energy. It can be observed that the clay ceramic is also subjected to dehydroxylation at temperatures between 450 and 600°C. The modification of the clay minerals, which is associated with a release of constitution water, involves a 169 J/g absorption of energy. Finally, the results show that the calcium carbonates from the clay mixture are subjected to decarbonation by the end of the firing process. This results in a 157 J/g adsorption of energy between 650 and 850°C. More details on the mineralogical transformations of the clay ceramic can be found in Nigay et al. (2017).

Concurrently, the MB<sub>50</sub> additive combusts in the clay ceramic from 250 to 450°C. The combustion results in a transformation of the PMMA into water and carbon dioxide. The exothermic reaction of combustion involves a 1,160 J/g release of energy during the firing process. It is important to note that this amount of energy, released in the form of heat, is greater than the amount of energy that is required by the firing transformations. In fact, the combustion of PMMA occurs on a free range of temperatures. The usual transformations of the clay are then not affected by the combustion of MB<sub>50</sub> additive. The MB<sub>10</sub> additive is subjected to combustion on the same range of temperature. The combustion of MB<sub>10</sub> additive also leads to a similar 1,143 J/g release of energy. This is due to the fact that MB<sub>10</sub> and MB<sub>50</sub> additives have a same composition of PMMA with yet a different particle size. The particle size of organic additives then has no effect on the thermal behavior of the clay ceramic. In fact, the thermal behavior of the clay ceramic only depends on the composition of the organic additives.

The mass loss of the clay ceramic is shown in Fig. 3. These results complete the previous results of the heat flow. In fact, the water release associated with the dehydration induces a mass loss of 3% by weight between 30 and 200°C. A mass loss of 2% by weight also results from the release of constitution water during the dehydroxylation at temperatures between 450 and 600°C. The release of carbon dioxide associated with the decarbonation also leads to a mass loss of 4% by weight between 650 and 850°C. Therefore, the clay ceramic is subjected to a mass loss of 9% by weight during the entire process of firing at temperatures up to 950°C.

The results of the mass loss also confirm the previous results of the thermal behavior of the MB<sub>50</sub> additive in the clay ceramic. In fact, the release of water and carbon dioxide associated with

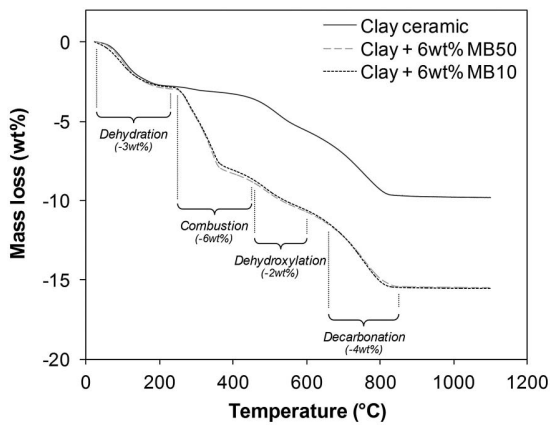


**Fig. 3.** Mass loss of the clay ceramic and of the clay ceramic with a 6% by weight addition of MB<sub>50</sub> and MB<sub>10</sub> additives

the combustion of the MB<sub>50</sub> additive induces a mass loss of 6% by weight at temperatures between 250 and 450°C. The 6% by weight loss corresponds to the 6% by weight addition of MB<sub>50</sub> in the clay ceramic. This means that the combustion of PMMA induces a full elimination of the MB<sub>50</sub> additive. The MB<sub>50</sub> additive is fully eliminated as a result of the pure organic nature of PMMA. The MB<sub>10</sub> additive is subjected to a same combustion as the MB<sub>50</sub> additive during the firing process. The combustion of the MB<sub>10</sub> additive also leads to a same mass loss as the combustion of the MB<sub>50</sub> additive. Hence, the particle size of the organic additives has no effect on the mass loss of the clay ceramic. The mass loss only depends on the percentage of organic additives along with their organic fraction.

The deformation of the clay ceramic is shown in Fig. 4. The results indicate that the clay ceramic without organic additives is subjected to shrinkage during the dehydration. In fact, the water release associated with the dehydration results in a 0.1% by volume shrinkage of the clay ceramic from 30 to 200°C. From 450 to 600°C, the dehydroxylation of the clay minerals induces a 0.1% by volume expansion of the clay ceramic. A sharp expansion of 0.3% is also associated with the  $\alpha \rightarrow \beta$  quartz inversion at around 600°C. It is important to note that the reverse transformation that occurs during the cooling induces a formation of major defects with the larger shrinkage of quartz than clay particles (Tarvornpanich et al. 2008).

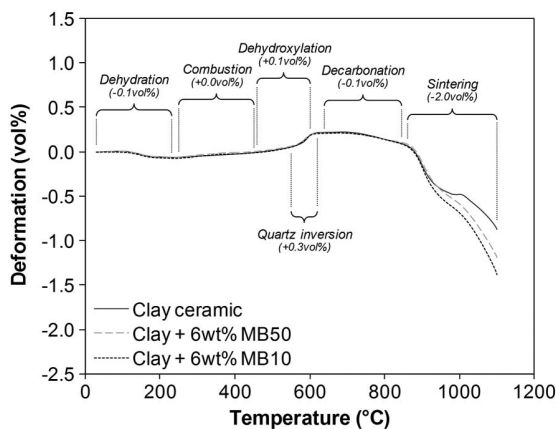


**Fig. 4.** Deformation of the clay ceramic and of the clay ceramic with a 6% by weight addition of MB<sub>50</sub> and MB<sub>10</sub> additives

Finally, the sintering induces an important shrinkage of the clay ceramic with the formation of necks between the clay particles. The shrinkage is still limited to 2% by volume owing to the decarbonation of calcium carbonates at temperatures up to 850°C.

The MB<sub>50</sub> additive is subjected to combustion in the clay ceramic at temperatures between 250 and 450°C. However, the combustion of the MB<sub>50</sub> additive does not result in any deformation of the clay ceramic. The deformation is not affected by the combustion of the MB<sub>10</sub> additive either in this range of temperatures. In fact, the organic additives only lead to a slight increase of the shrinkage during the sintering process. The shrinkage is increased by 0.3% by volume in the case of a 6% by weight addition of MB<sub>50</sub> additives. Similarly, the 6% by weight addition of MB<sub>10</sub> additives induces a 0.5% by volume increase of the shrinkage. The deformation of the clay ceramic is then not significantly affected by the particle size distribution of the organic additives. Furthermore, this slight increase of the shrinkage occurs at temperatures between 950 and 1,100°C. This means that the organic additives do not induce any deformation of the clay ceramic at the standard temperature of firing (i.e., 950°C). Overall, the clay ceramic is only affected by the mass loss of the organic additives, which depends on the percentage of addition and their organic fraction.

### Microstructure of the Clay Ceramic

The porosity of the clay ceramic is presented in Fig. 5. It can be observed that the clay ceramic without organic additives has a volume fraction of pores equal to 24% by volume (bulk density of 2,061 kg · m<sup>-3</sup>) prior to firing (i.e., at 30°C). In fact, the air remaining in the clay ceramic mixture is trapped in the form of pores during the extrusion. This porosity also increases with the water release during the drying process. Moreover, the dehydration of the clay ceramic induces a 2% by volume formation of porosity from 30 to 200°C (decrease of the bulk density from 2,061 to 2,011 kg · m<sup>-3</sup>). The porosity also increases by 2% by volume during the dehydroxylation at temperatures between 450 and 600°C (decrease of the bulk density from 1,996 to 1,955 kg · m<sup>-3</sup>). The decarbonation of the calcium carbonates also results in a 3% by volume formation of porosity between 650 and 850°C (decrease of the bulk density from 1,943 to 1,876 kg · m<sup>-3</sup>). In fact, the porosity only decreases by 2% by volume during the sintering from 850 to 1,100°C (increase of the bulk density from 1,876 to 1,927 kg · m<sup>-3</sup>). This means that the clay ceramic conserves a porosity of 30% by volume (bulk density of 1,902 kg · m<sup>-3</sup>) after firing at 950°C.

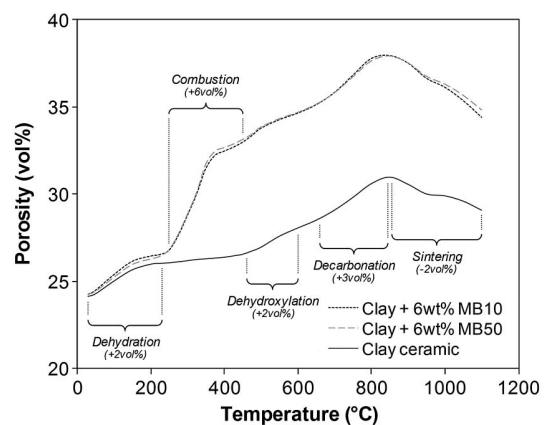


**Fig. 5.** Porosity of the clay ceramic and of the clay ceramic with a 6% by weight addition of MB<sub>50</sub> and MB<sub>10</sub> additives

The combustion of the 6% by weight of MB<sub>50</sub> additive induces a 6% by volume increase of the porosity (decrease of the bulk density from 1,928 to 1,814 kg · m<sup>-3</sup>). It was shown previously that the combustion of MB<sub>50</sub> additive does not induce any deformation of the clay ceramic. Hence, the porosity formation of the clay ceramic results from the mass loss of the MB<sub>50</sub> additive. The porosity formation occurs on the free range of temperature from 250 to 450°C. Therefore, the porosity formations associated with the clay transformations are not modified by the porosity formation associated with the combustion of MB<sub>50</sub>. It is important to note that the porosity resulting from the combustion of MB<sub>50</sub> is added and conserved up to 1,100°C. This means that the porosity has an additive and conservative behavior during the entire process of firing. The MB<sub>10</sub> additive results in a same formation of porosity because its combustion induces a same mass loss (6% by weight) as the combustion of MB<sub>50</sub> additive. The particle size of the organic additives has no effect on the porosity of the clay ceramic. The porosity depends on the mass loss of the organic additives during the firing process. The percentage of porosity is then controlled by the percentage of organic additives along with their organic fraction.

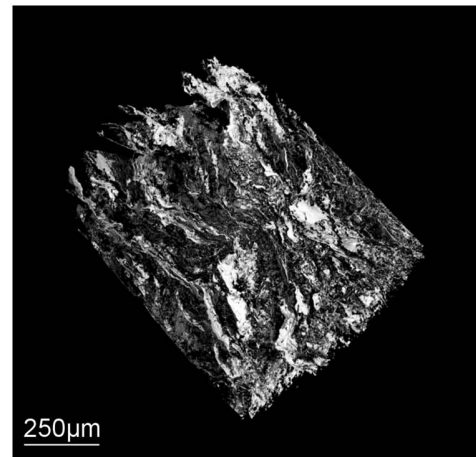
The 3D representation of the porosity is presented in Fig. 6. The clay ceramic without organic additives has a microstructure of clay with porosity sheets. As shown by Korah et al. (2016), the clay is compressed in the form of sheets during the extrusion. The air remaining in the clay mixture is then compressed as porosity sheets between the sheets of clay. It is important to note that the porosity sheets forming during the extrusion are not eliminated by the formation of pores during the firing. The large sheets of porosity that correspond to major defects are also conserved during the sintering up to 950°C.

The clay ceramic with a 6% by weight addition of MB<sub>50</sub> additives does not contain any sheets of porosity. In fact, the MB<sub>50</sub> additive induces an elimination of the porosity sheets soon after the extrusion process. The small particles of MB<sub>50</sub> additive increase the compression of the clay. Therefore, the air remaining in the clay mixture is compressed between the sheets of clay in the form of smaller pores during the extrusion process. The clay ceramic with a 6% by weight addition of MB<sub>50</sub> additive also contains spherical pores with a 50 μm diameter. The 50-μm diameter of these pores corresponds to the 50-μm size of the MB<sub>50</sub> additive. Hence, these pores represent the 6% by volume formation of porosity resulting from the combustion of MB<sub>50</sub> additive during the firing process. The pores associated with the combustion of the organic additive represent the voids released by their particles in the microstructure.

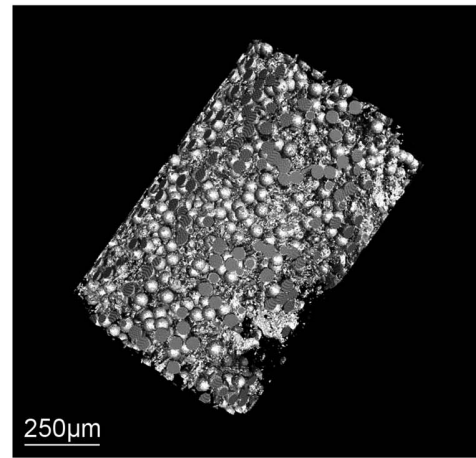
The clay ceramic with a 6% by weight addition of MB<sub>10</sub> additives does not contain any sheets of porosity. Moreover, the 10-μm particles of MB<sub>10</sub> additive induce a formation of smaller 10-μm pores than those of MB<sub>50</sub> additive. It results in a larger reduction of the pore size diameter of the clay ceramic after the firing process. The type of porosity is eventually controlled by the particle size of the organic additives. On the other hand, the organic fraction of the additives provides a control of the percentage of porosity.

### Thermal Properties of the Clay Ceramic

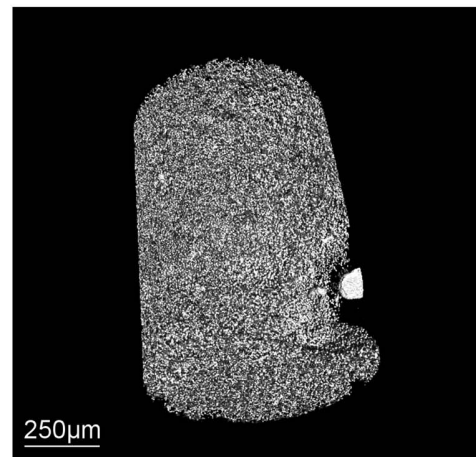
The dependence of the thermal conductivity on the firing temperature of the clay ceramic is presented in Fig. 7. The results show that the clay ceramic without organic additives has a thermal conductivity of 1.07 W/m · K prior to firing (i.e., at 30°C). As shown by Nigay et al. (2017), this value corresponds to a combination between the high thermal conductivity of the clay and the low thermal conductivity of air in the porosity sheets. The impact of air is also enhanced in this direction of the thermal gradient of the walls with the anisotropy of the porosity sheets. The thermal conductivity



(a)



(b)



(c)

**Fig. 6.** X-ray tomography representation of (a) porosity of the clay ceramic; clay ceramic with a 6% by weight addition of (b) MB<sub>50</sub> additive and (c) MB<sub>10</sub> additive

decreases by 30% during the firing process of the clay ceramic up to 850°C. The decrease is associated with the 7% by volume formation of porosity due to the dehydration, dehydroxylation, and decarbonation. In fact, the thermal conductivity decreases as a result of the low thermal conductivity of air in the newly formed pores. The thermal conductivity only increases with the sintering

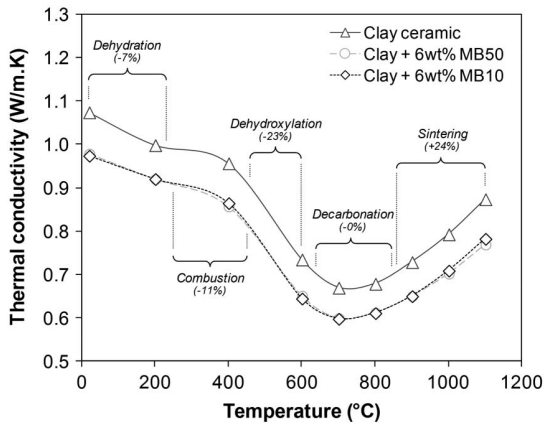


**Fig. 7.** Dependence of the thermal conductivity on the firing temperature of the clay ceramic and of the clay ceramic with a 6% by weight addition of MB<sub>50</sub> and MB<sub>10</sub> additives

up to 1,100°C. The greater fraction of clay results in a 24% increase of the thermal conductivity.

The 6% by weight addition of MB<sub>50</sub> additive induces an 11% decrease of the thermal conductivity prior to firing (i.e., at 30°C). The thermoplastic polymer of PMMA has, in accordance with the literature, a relatively low thermal conductivity. Hence, the insulating behavior of MB<sub>50</sub> additive decreases the thermal conductivity of the clay ceramic soon after the extrusion process. The combustion of MB<sub>50</sub> additive leads to a 6% by volume increase of the porosity between 250 and 450°C. However, the newly formed pores do not induce a significant decrease of the thermal conductivity. The thermal conductivity of air in the newly formed pores is equivalent to that of the PMMA. The impact of the porosity on the thermal conductivity of the clay ceramic is then all provided during the extrusion process. But, the transformation of MB<sub>50</sub> additive into porosity allows a conservation of the initial decrease of the thermal conductivity. The porosity has indeed an additive and a conservative behavior on the entire process of firing. The 11% decrease of the thermal conductivity during the extrusion process is then conserved during the firing process up to 1,100°C.

The 6% by weight addition of MB<sub>10</sub> additive results in a same decrease of the thermal conductivity as that of MB<sub>50</sub> additive during the extrusion. The combustion of the MB<sub>10</sub> additive also results in a same conservation of the initial decrease in the thermal conductivity during the firing. This means that the particle size of the organic additives has no effect on the thermal conductivity. The thermal conductivity of the clay ceramic is related to the percentage of porosity after firing. Therefore, the thermal conductivity is controlled by the percentage of organic additives along with their organic fraction.

### Mechanical Properties of the Clay Ceramic

The dependence of the Young's modulus on the firing temperature of the clay ceramic is shown in Fig. 8. The results indicate that the clay ceramic without organic additives has a Young's modulus of 7.5 GPa prior to firing (i.e., at 30°C). This value results from the formation of clay sheets during the extrusion. However, it is also minimized by the large sheets of porosity which are acting as defects. The firing process does not induce a significant decrease of the Young's modulus at temperatures between 30 and 850°C. The dehydration, dehydroxylation and decarbonation leads to a porosity formation of 7% by volume in this range of temperatures. But, the pores associated with the firing transformations are smaller than the

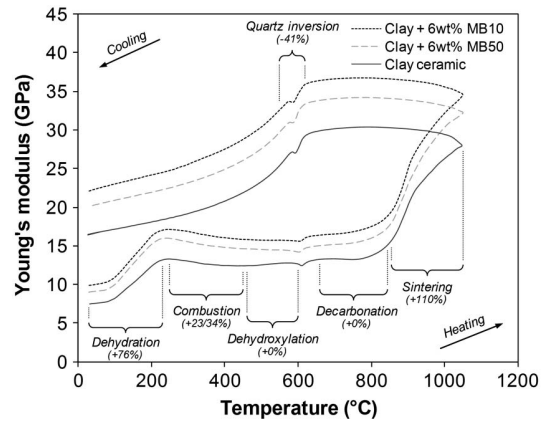


**Fig. 8.** Dependence of the Young's modulus on the firing temperature of the clay ceramic and of the clay ceramic with a 6% by weight addition of MB<sub>50</sub> and MB<sub>10</sub> additives

large porosity sheets from the extrusion. This result suggests that a formation of smaller pores than the defects of the microstructure allows a conservation of the Young's modulus. On the other hand, the densification results in a 110% increase of the Young's modulus between 850 and 1,050°C. This means that the Young's modulus only decreases with the  $\beta \rightarrow \alpha$  quartz inversion during the cooling.

The 6% by weight addition of MB<sub>50</sub> additive induces a 23% increase of the Young's modulus prior to firing (i.e., at 30°C). The thermoplastic polymer of PMMA has no significant stiffness compared with the clay. However, the small particles of MB<sub>50</sub> additive reduce the pore size diameter of the clay ceramic. Hence, the smaller pores resulting from the extrusion have a lower impact on the Young's modulus. The Young's modulus is then increased by the MB<sub>50</sub> additive soon after the extrusion. The combustion of the MB<sub>50</sub> additive also leads to a 6% by volume formation of porosity during the firing process. But, the transformation of the MB<sub>50</sub> additive into pores does not decrease the Young's modulus. The Young's modulus is not decreased because the stiffness of the pores is equivalent to that of PMMA. The impact of the newly formed pores on the Young's modulus is then all provided during the extrusion process. However, the transformation of MB<sub>50</sub> additive into porosity allows a conservation of the initial increase of the Young's modulus. The porosity has indeed an additive and a conservative behavior on the entire process of firing. The 23% increase of the Young's modulus during the extrusion process is then conserved during heating and cooling.

The 6% by weight addition of MB<sub>10</sub> additive also results in an increase of the Young's modulus soon after extrusion. However, the MB<sub>10</sub> additive induces a greater increase of 34% due to a smaller 10- $\mu$ m size of the particles. This means that the particle size of the organic additives has a major impact on the Young's modulus. In fact, the Young's modulus depends on the percentage and the size of the pores after the firing process. The Young's modulus is then controlled by the percentage of organic additives along with their particle size distribution.

The flexural strengths of the clay ceramic after firing at 950°C are given in Table 2. The results confirm the impact of the particle size of the organic additives on the Young's modulus. The 50- $\mu$ m particles of the MB<sub>50</sub> additives induce a 26% increase of the flexural strength using a 6% by weight addition. The clay ceramic with a 6% by weight addition of MB<sub>50</sub> additives has then a flexural strength of 15.4 MPa after the firing process. On the other hand, the 6% by weight addition of MB<sub>10</sub> additive with smaller particles of 10  $\mu$ m results in a greater increase of the flexural strength by

**Table 2.** Flexural Strength of the Clay Ceramic and of the Clay Ceramic with a 6% by Weight Addition of MB<sub>50</sub> and MB<sub>10</sub> Additives

Samples	Flexural strength (MPa)
Clay ceramic	12.2 ± 0.2
Clay + 6% by weight MB <sub>10</sub>	15.4 ± 0.2
Clay + 6% by weight MB <sub>50</sub>	16.2 ± 0.1

33%. The clay ceramic then has a flexural strength of 16.2 MPa using a 6% by weight addition of MB<sub>10</sub> additive.

### Energy Balance of the Clay Ceramic

The energy balance of the clay ceramic is given in Table 3. The results indicate a 1,144 J/g release of energy for a 6% by weight addition of MB<sub>10</sub> additive. This value corresponds to the amount of heat that is released by the combustion of PMMA during the firing process. In fact, it is equal to the lower heating value of the PMMA sample (i.e., 23,291 J/g) weighted by its percentage of addition (i.e., 6% by weight) in the clay ceramic. This means that the entire amount of energy from PMMA is released during the firing process. The MB<sub>50</sub> additive has a same pure organic nature as the MB<sub>10</sub> additive. Hence, the 6% by weight addition of MB<sub>50</sub> additive induces a same release of 1,160 J/g. The amount of energy released during the firing process is then related to the percentage of organic additive along with their organic fraction.

The firing process of the clay ceramic involves 1,550 J/g of energy. This value corresponds to the amount of energy required to reach the firing temperature of 950°C, in addition to the amount of energy absorbed by the clay transformations. The increase of the temperature from 30 to 950°C requires 920 J/g of energy. On the other hand, 630 J/g of energy is absorbed by the dehydration, dehydroxylation, and decarbonation reactions at temperatures up to 950°C. The combustion of MB<sub>10</sub> and MB<sub>50</sub> additives does not induce any modification of the clay transformations. Therefore, the firing process of the clay ceramic with organic additives also requires 1,550 J/g of energy.

The amount of energy released by the combustion of MB<sub>10</sub> additive covers 73.8% of the amount of energy required by the firing process. The MB<sub>50</sub> additive provides a same energetic contribution of 74.8%. Therefore, the particle size of the organic additives has no apparent effect on the energetic contribution. The energetic contribution is related to the percentage of organic additive with their organic fraction. A greater addition of such pure organic additives could cover the entire amount of energy required by the firing process. This means that the use of small organic additives as pore-forming agents in clay ceramics can provide both an improvement of the thermal/mechanical properties and extensive energy savings.

### Implications

The implications of this research are significant in the field of building materials. The building materials, such as fired clay bricks, are

**Table 3.** Energy Balance of the Clay Ceramic with a 6% by Weight Addition of MB<sub>50</sub> and MB<sub>10</sub> Additives

Samples	Energy released (J/g)	Energy required (J/g)	Contribution (%)
Clay + 6% by weight MB <sub>10</sub>	1,144	1,550	73.8
Clay + 6% by weight MB <sub>50</sub>	1,160	1,550	74.8

used for their thermal and mechanical properties. The literature has shown an improvement of the thermal properties using organic wastes as pore-forming agents. The thermal conductivity of the fired clay bricks decreased by 18 (Aouba et al. 2016) up to 51% (Kadir and Mohajerani 2011) with a 5% by weight addition of olive stone flour or cigarette butts. However, the improvement of the thermal properties was associated with a decrease in the mechanical properties. The compressive strength of the bricks with a 5% by weight addition of olive stone flour or cigarette butts decreased by 31 up to 80%.

In this study, the thermal and mechanical properties of a clay ceramic used for building applications were improved at the same time using organic additives with a small particle size. The 6% by weight addition of small organic additives decreased the thermal conductivity by 11%. This decrease in the thermal conductivity is slightly lower than that obtained in the literature (18–51%). Nevertheless, it was associated with a 33% increase of the flexural strength. This improvement of the mechanical properties is a step forward compared with the different losses that are observed in the literature (30–80%). In fact, it suggests that the thermal and mechanical properties of fired clay bricks can be improved by the addition of many organic wastes using a preliminary reduction of their particle size.

The amount of energy that was released by the combustion of the organic additives also covered 73.8% of the amount of energy required by the firing. Therefore, the use of small organic additives as pore-forming agents provides an improvement of the performances as well as energy savings in the clay bricks industry. This reduces greenhouse gases emissions and contributes toward the objectives of reducing the impact of building materials on the global environment.

### Conclusions

This research investigated the impact of the particle size distribution of organic additives on the microstructure of a clay ceramic and its thermal and mechanical properties. The impact of the particle size distribution was elucidated by the addition of a thermoplastic polymer in one form of 10- $\mu\text{m}$  particles and one form of 50- $\mu\text{m}$  particles. In fact, the organic additives were subjected to combustion during firing of the clay ceramic. The combustion occurred on a free range of temperatures between 250 and 450°C. The reactions of the clay were then not modified by the combustion of the organic additives.

The transformation of the organic additives into water and carbon dioxide resulted in a porosity formation. The porosity was conserved during the firing process up to 950°C. Moreover, the pore size diameter of the clay ceramic corresponded to the particle size distribution of the organic additives. The impact of the organic additives on the thermal and mechanical properties of the clay ceramic was then conserved in the form of porosity after firing.

The 10- and 50- $\mu\text{m}$  pores resulting from the combustion of the organic additives induced a same decrease in the thermal conductivity. In fact, the thermal conductivity depended on the percentage of porosity. The thermal conductivity was then controlled by the percentage of organic additives along with their organic fraction. However, the 10- $\mu\text{m}$  pores induced a greater increase of the Young's modulus and of the flexural strength than the 50- $\mu\text{m}$  pores. In fact, the Young's modulus and the flexural strength depended on the percentage of porosity as well as the pore size diameter. The mechanical properties were then controlled by the percentage of organic additives along with their organic fraction and their particle size.



## Acknowledgments

The authors would like to acknowledge the TERREAL Company for financial support and scientific contribution to this study. We also thank the staff of the ICA and RAPSODEE Research Centers at Ecole des Mines d'Albi for its assistance with the research.

## References

- Andreola, F., Barbieri, L., Corradi, A., Lancellotti, I., and Manfredini, T. (2001). "The possibility to recycle solid residues of the municipal waste incineration into a ceramic tile body." *J. Mater. Sci.*, 36(20), 4869–4873.
- Aouba, L., Bories, C., Coutand, M., Perrin, B., and Lemerrier, H. (2016). "Properties of fired clay bricks with incorporated biomasses: Cases of olive stone flour and wheat straw residues." *Constr. Build. Mater.*, 102(1), 7–13.
- ASTM International. (2010). "Standard test methods for flexural properties of unreinforced and reinforced plastics and electrical insulating materials." *ASTM D790-10*, West Conshohocken, PA.
- Baillez, S., and Nzihou, A. (2004). "The kinetics of surface area reduction during isothermal sintering of hydroxyapatite adsorbent." *Chem. Eng. J.*, 98(1–2), 141–152.
- Bánhidi, V., and Gömze, L. A. (2008). "Improvement of insulation properties of conventional brick products." *Mater. Sci. Forum*, 589, 1–6.
- Bories, C., Aouba, L., Vedrenne, E., and Vilarem, G. (2015). "Fired clay bricks using agricultural biomass wastes: Study and characterization." *Constr. Build. Mater.*, 91, 158–163.
- Bories, C., Borredon, M. E., Vedrenne, E., and Vilarem, G. (2014). "Development of eco-friendly porous fired clay bricks using pore-forming agents: A review." *J. Environ. Manage.*, 143, 186–196.
- Demir, I. (2008). "Effect of organic residues addition on the technological properties of clay bricks." *Waste Manage.*, 28(3), 622–627.
- Dondi, I., Mazzanti, F., Principi, P., Raimondo, M., and Zanarini, G. (2004). "Thermal conductivity of clay bricks." *J. Mater. Civ. Eng.*, 10.1061/(ASCE)0899-1561(2004)16:1(8), 8–14.
- Ducman, V., and Kopar, T. (2001). "Sawdust and papermaking sludge as pore-forming agents for lightweight clay bricks." *Ind. Ceram.*, 21(2), 81–86.
- Eliche-Quesada, D., Martínez-Martínez, S., Pérez-Villarejo, L., Iglesias-Godino, F. J., Martínez-García, C., and Corpas-Iglesias, F. A. (2012). "Valorization of biodiesel production residues in making porous clay brick." *Fuel Process. Technol.*, 103, 166–173.
- Kadir, A. A., and Mohajerani, A. (2011). "Recycling cigarette butts in lightweight fired clay bricks." *Constr. Mater.*, 164(5), 219–229.
- Korah, L. V., Nigay, P. M., Cutard, T., Nzihou, A., and Thomas, S. (2016). "The impact of the particle shape of organic additives on the anisotropy of a clay ceramic and its thermal and mechanical properties." *Constr. Build. Mater.*, 125, 654–660.
- Mendivil, M. A., Muñoz, P., Morales, M. P., Letelier, V., and Juárez, M. C. (2017). "Grapevine shoots for improving thermal properties of structural fired clay bricks: New method of agricultural-waste valorization." *J. Mater. Civ. Eng.*, 10.1061/(ASCE)MT.1943-5533.0001892, 04017074.
- Mohajerani, A., Kadir, A. A., and Larobina, L. (2016). "A practical proposal for solving the world's cigarette butt problem: Recycling in fired clay bricks." *Waste Manage.*, 52, 228–244.
- Monteiro, S. N., Alexandre, J., Margem, J. I., Sánchez, R. J., and Vieira, C. M. F. (2008). "Incorporation of sludge from water treatment plant into red ceramic." *Constr. Build. Mater.*, 22(6), 1281–1287.
- Monteiro, S. N., and Vieira, C. M. F. (2014). "On the production of fired clay bricks from waste materials: A critical update." *Constr. Build. Mater.*, 68, 599–610.
- Muñoz Velasco, P., Ortiz, M. P., Giró, M. A., Melia, D. M., and Rehbein, J. H. (2015). "Development of sustainable fired clay bricks by adding kindling from vine shoot: Study of thermal and mechanical properties." *Appl. Clay Sci.*, 107, 156–164.
- Nigay, P. M., Cutard, T., and Nzihou, A. (2017). "The impact of heat treatment on the microstructure of a clay ceramic and its thermal and mechanical properties." *Ceram. Int.*, 43(2), 1747–1754.
- Phonphuak, N., and Chindapasirt, P. (2014). "Types of waste, properties, and durability of pore-forming waste-based fired masonry bricks." *Eco-efficient masonry bricks and blocks: Design, properties and durability*, F. Pacheco-Torgal, P. B. Lourenço, J. A. Labrincha, P. Chindapasirt, and S. Kumar, eds., Woodhead Publishing, Cambridge, U.K., 103–127.
- Tarvornpanich, T., Souza, G. P., and Lee, W. E. (2008). "Microstructural evolution in clay-based ceramics. II: Ternary and quaternary mixtures of clay, flux, and quartz filler." *J. Am. Ceram. Soc.*, 91(7), 2272–2280.
- Ukwatta, A., and Mohajerani, A. (2017). "Effect of organic content in biosolids on the properties of fired-clay bricks incorporated with biosolids." *J. Mater. Civ. Eng.*, 10.1061/(ASCE)MT.1943-5533.0001865, 04017047.
- Zhang, L. (2013). "Production of bricks from waste materials—A review." *Constr. Build. Mater.*, 47, 643–655.